Zeitschrift: Schweizerische mineralogische und petrographische Mitteilungen = Bulletin suisse de minéralogie et pétrographie

Band: 77 (1997)

Heft: 3

Artikel: Metamorphosed Precambrian mafic rocks from the South Carpathians : island arc remnants? A geochemical characterization of amphibolites from the Fgra Mountains, Romania

Autor: Drguanu, Cristian / Tanaka, Tsuyoshi / Iwamori, Hikaru

DOI: https://doi.org/10.5169/seals-58494

SCHWEIZ. MINERAL. PETROGR. MITT. 77, 419–437, 1997

Metamorphosed Precambrian mafic rocks from the South Carpathians: island arc remnants? A geochemical characterization of amphibolites from the Făgăraș Mountains, Romania

by *Cristian Drăguşanu*[1], *Tsuyoshi Tanaka*[1] and *Hikaru Iwamori*[1]

Abstract

This work describes general geochemical features of the Precambrian mafic rocks, mainly amphibolites which occur extensively in two metamorphic formations of the Cumpăna Group, an important tectonic block incorporated in the Carpathian Belt. Direct and inverse approaches relate the behavior of major and 29 minor, incompatible and compatible elements with the geological environment.

The statistical regression of the major element concentrations confirmed the two models according to which most of the amphibolites have originated from basaltic magmas, but at the same time a part of them were derived from mechanical mixtures of a similar igneous component and crustal sediments. The compositions of the possible parental liquids of the least fractionated sample, corrected for olivine crystallization, were in equilibrium with mantle between 15 and 22 kb.

The REE modeling requires around 5% partial melting of a depleted mantle, initiated in the garnet stability field, possible to exist in hydrous conditions. Furthermore, 20–90% fractional crystallization of a clinopyroxene rich solid and its partial remelting can determine the observed REE abundances and chondrite normalized patterns. The HFSE elemental ratios are characteristic of tholeiitic basalts. On the average, the amphibolites are depleted in Nb and Zr, which is a geochemical feature of continental or island arc tectonic settings.

The distribution of transition metal abundances is consistent with the assumption that some parts of the stratigraphic sequence are potential hosts for terrigenous mixing processes. The strato-volcanic structure identified in the lithostratigraphic Group of Cumpăna can be related with the presence of an incipient island arc.

Keywords: amphibolite, basaltic magma, geochemistry, trace element partitioning, assimilation, island arc environment, South Carpathians, Romania.

Introduction

In the Carpathians, as is also the case alongside the Alpine Belt, isolated rocks and structures of Precambrian and Paleozoic age are common, leading to intriguing questions about their origin which is mostly obscured by Paleozoic metamorphic events. The mafic rocks are the best candidates for geochemical fingerprinting of deep processes. They may offer suggestions about the mechanisms of their geological setting, in an area which possibly remained unstable and determined a very long period of tectonic activity, known as Alpine orogeny. In the late Miocene, the Carpathians were uplifted in very large recumbent folds. The South Carpathians comprise three major nappe complexes formed due to the continental collision during the Upper Jurassic-Cretaceous and then overthrusted onto the Moesian Platform during the Miocene. Shown in figure 1, structurally upwards they are: the Danubian nappe system (BERZA et al., 1983), the Getic nappe system (MUNTEANU-MURGOCI, 1907) and the Supragetic nappe system (STRECKEISEN, 1934).

In the Alpine tectonic frame of the South Carpathians, the general geology of the Făgăraș Mountains is well known, by the works of

[1] Department of Earth and Planetary Sciences, Nagoya University, Nagoya 464-01, Japan. E-mail: cris@pikaru.eps.nagoya-u.ac.jp.

PRIMIČS (1884) from DIMITRESCU (1964), GHIKA-BUDEȘTI (1940), MANILICI (1955), DIMITRESCU (1964, 1978, 1988), DIMITRESCU et al. (1978, 1985). According to BALINTONI et al. (1986) the Făgăraș Mountains are built up of Austrian tectonic units and post tectonic sedimentary covers. One of these, the Argeș Nappe is well exposed on the southern slope. Its basement consists of Precambrian metamorphic formations, belonging to the lithostratigraphic group of Cumpăna, which includes mafic rocks. KRÄUTNER (1980) assigned the Cumpăna Group as a part of the Carpian Supergroup consisting of the oldest rocks known in the Romanian Carpathians. It corresponds to the lower cycle of the Upper Precambrian (Middle Proterozoic) known elsewhere under different names as pre-Baikalian, pre-Assyntian, Grenvillian or more frequently Dalslandian.

The geochemical data of the constituent rocks from this area are rather poor, generally restricted to major elements and some trace elements compositions. UDUBAȘA et al. (1988) gave a description of a metamorphosed copper-nickel mineralization hosted in a lenslike mafic sequence

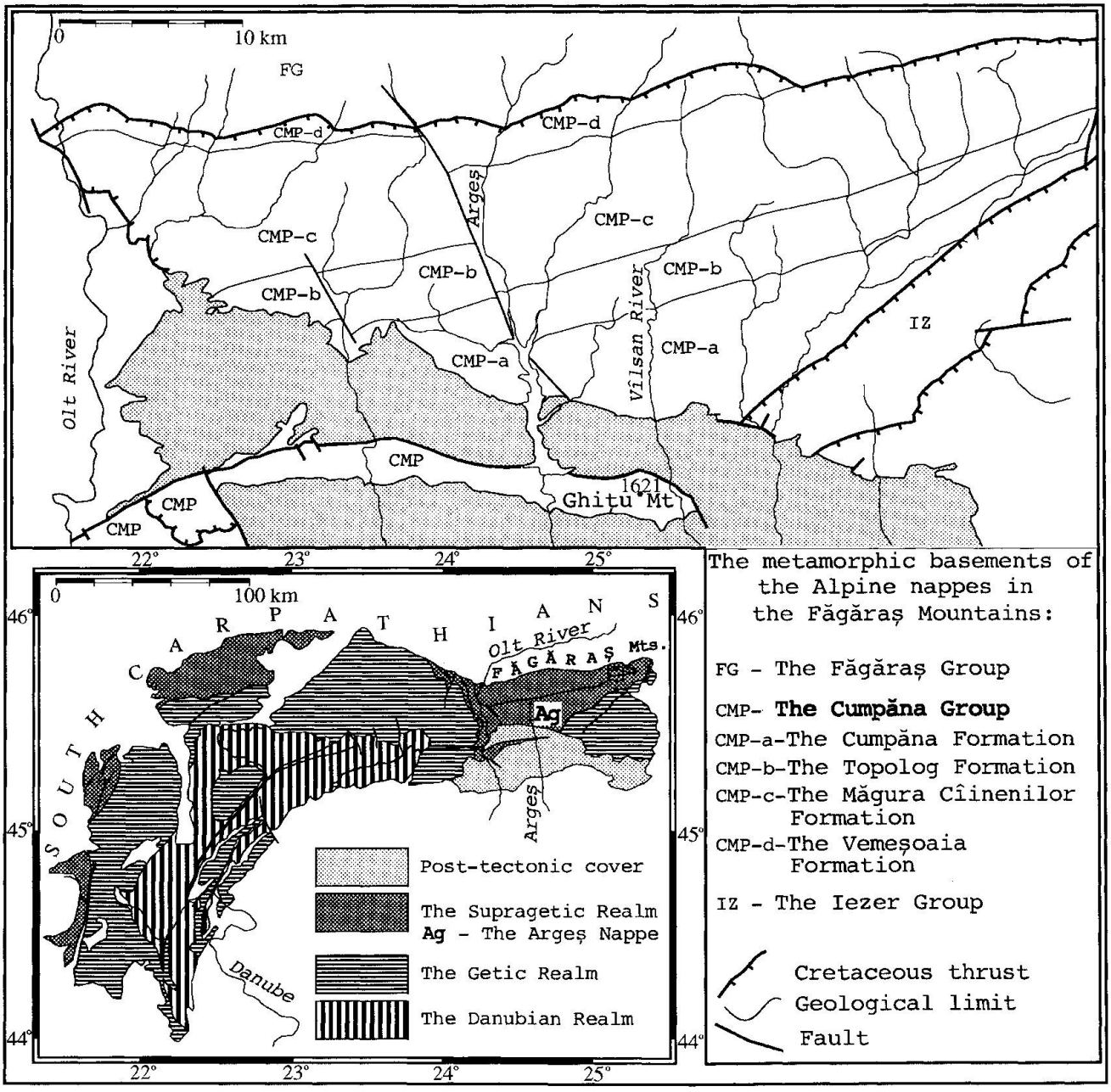

Fig. 1 Tectonic sketch showing the position of the Argeș Nappe in the frame of South Carpathians and the most complete lithostratigraphic sequence of its basement, the Cumpăna Group (SĂNDULESCU, 1984; DIMITRESCU et al., 1985; BALINTONI et al., 1986; GHEUCĂ, 1988; BERZA et al., 1994).

from the Vîlsan Valley, related to the Precambrian metamorphics from the Ghiţu Mountains (Fig. 1). The rocks were described as part of an ophiolitic series. Their original gabbroic character was masked by progressive metamorphic events, within the limits of the amphibolite facies and retrograde metamorphism in the greenschist facies. In the described succession, the ultramafic parts of the magmatic complex have not been found yet, probably as consequence of their tectonic mobility. On the other hand, in the Zîrna Valley (Fig. 2), GANDRABURA et al. (1992) found a succession of metaultramafites, ortho- and para-amphibolites. Their approach, based on the geochemical association of trace elements, suggested the involvement of the same magmatic component in the protolith of the amphibolites.

Outline of geology and petrography

The lithostratigraphic group named Cumpăna is an ENE–WSW trending monocline dipping steeply southwards (BALINTONI et al., 1986).

Four main constituent formations occur in stratigraphic succsession, from south to north (DIMITRESCU et al., 1985, GHEUCĂ, 1988, Fig. 1, Fig. 2):

a) The Cumpăna Formation includes augen gneisses, migmatites, paragneisses and amphibolites.

b) The Topolog Formation is an alternation of paragneisses, augen gneisses, quartzo-feldspathic gneisses, amphibolites and micaschists.

c) The Măgura Cîinenilor Formation consists mainly of micaschists.

d) The Vemeşoaia Formation begins with 1–3 bands of carbonatic rocks, followed by quartzitic paragneisses.

A NW–SE striking, highly inclined fault system, corresponding to the Alpine folding events, cuts the area into small compartments with related mylonitization and alteration. Connected with this fragmentation, discordant to the structure, small dolerite dykes occur.

Our area of investigation concerns two of the above formations: the Cumpăna Formation and the Topolog Formation.

In the Cumpăna Formation, which has the lowest stratigraphic position in the Cumpăna Group, the amphibolites form thick concordant layers or lenses ranging from a few meters to a few hundred meters in size. They exhibit massive, granoblastic-nematoblastic or heterogranular textures. The highest *P-T* metamorphic event, corresponding to the facies of amphibolites with almandine, obliterated most of the original texture, although relics of gabbroic textures can be recognized. The amphibole, which is in most of the cases a hornblende-tschermakitic hornblende, prevails representing around 70% of rock mass. It may coexist with tremolite which tends to be the major mineral constituent in the eastern part of the studied area. This can be the result of a replacement in different stages of the prograde metamorphism. The mineral parageneses of the hornblende amphibolites and tremolite amphibolites are quite similar and consist of plagioclase, chlorite, biotite, ± garnet and small proportions of apatite, zircon, ± clinopyroxenes, carbonates, ilmenite, ± zoisite, ± rutile, ± magnetite, ± pyrrhotite, ± sphene, ± quartz. Anthophyllite was found in a very magnesian rock, sample 1, and it is thus thought to be related to an ultramafic parental material. The associated mineral assemblage consists of plagioclase, serpentine, and small proportions of clinopyroxene, orthopyroxene, ilmenite, zoisite, rutile, magnetite, and pyrrhotite. The neighboring rock of the amphibolites and also the predominant rock in the area is an augen gneiss. It has a modal composition of 25–45% microcline, 15–35% plagioclase (An_{20-30}), 10–30% quartz, 5–15% biotite, 0–4% muscovite, 1% garnet, 1% epidote and clinozoisite, 1% chlorite.

In the Topolog Formation, the amphibolites show a clear foliation and the variation in thickness is between a few centimeters and a few tens of meters. Frequently, they exhibit a banded texture, which consists of an alternation of amphibole rich and plagioclase rich zones. The gradation between coarse and fine minerals or between mafic and felsic parts, which is frequently observed, is strong support for their sedimentary origin. The main mineral constituents are green hornblende, plagioclase (An_{15-20}) and small amounts of almandine, magnetite, ilmenite, pyrite and quartz. Anthophyllite occurs incidentally and may be an argument for an eventual mixing process with igneous material. The host rock is usually a paragneiss, that may contain biotite, with amphibole, biotite and graphite, or with amphibole and garnet. Augen gneisses of the same mineral assemblages as described in the Cumpăna Formation occur in smaller areas and are less frequently associated with amphibolites.

Taking an overview of the two formations to be examined, an alternation of amphibolites with quartzofeldspathic rocks (leptynites) is the characteristic rock association. Most of the authors agree that it is a type of volcano-sedimentary formation (KRÄUTNER, 1980). The Cumpăna Group exhibits a continuous lithological sequence from concordant mafic rocks, possibly associated with ultramafites (if we consider those found by GAN-

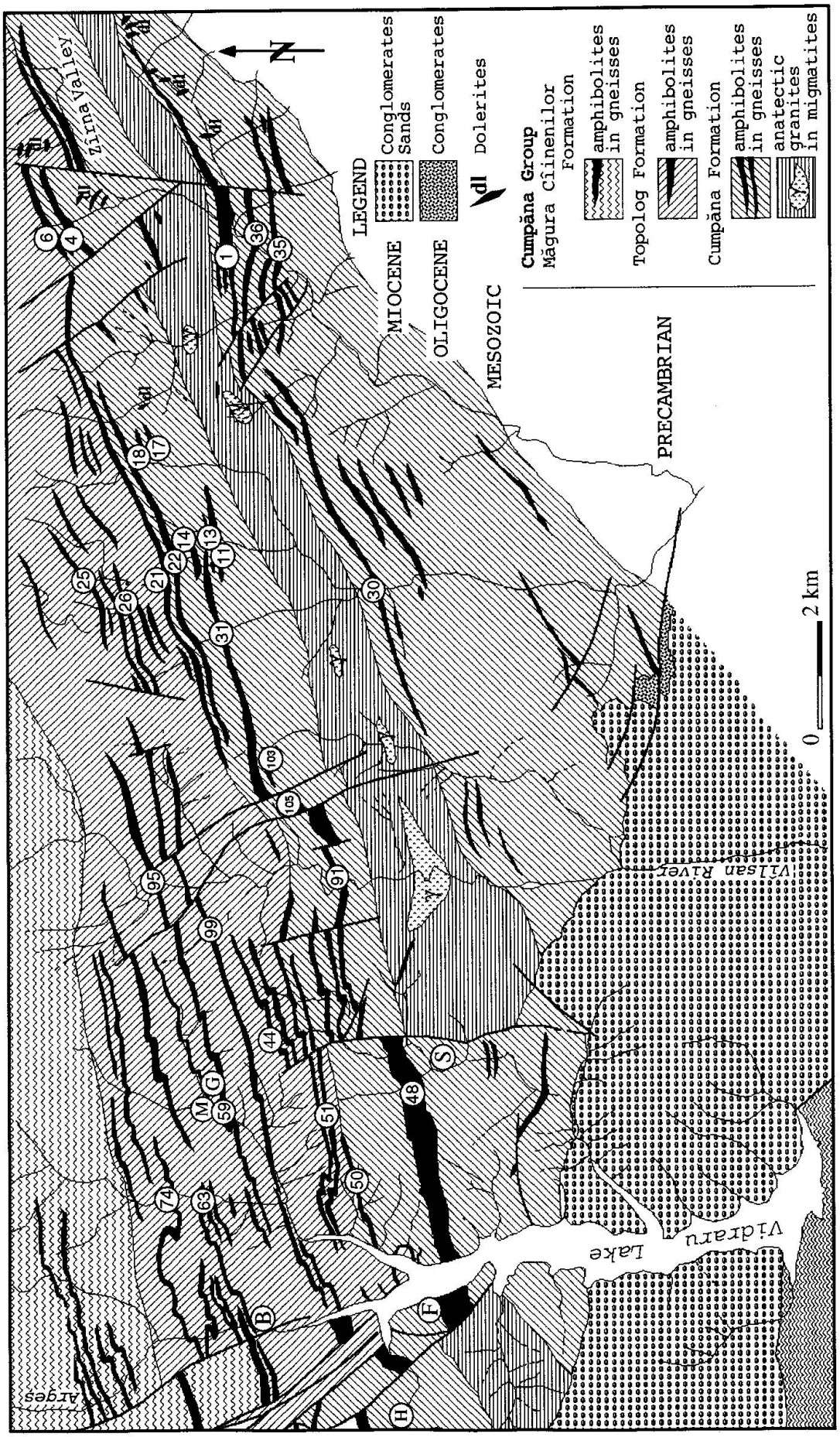

Fig. 2 Geological map (after DIMITRESCU et al., 1985), showing the location of samples (circles with numbers or letters).

DRABURA et al., 1992 and one found by us), metasedimentary rocks up to carbonatic rocks. It seems stratigraphically unitary and yet no discordant limit has been identified inside the pile. For these reasons, this geological frame must have preserved most of its original structure. There is no evidence for which a change of the tectonic environment and implicitly of the magmatic source should be considered.

Considerations on possible chemical disturbances during metamorphism

From the point of view of mineral assemblages, it is not easy to observe whether there is a polyphasic character of these metamorphics, since structural and mineralogical re-equilibration could have taken place (UDUBAŞA et al., 1988). According to the preliminary observations of UDUBAŞA et al. (1994), based on the Al-in-hornblende barometer, the garnet-biotite geothermometer and the Si-in-phengite barometer, a prograde evolution within the epidote-amphibolite facies at $P = 5–7.5$ kbar and $T = 500–650$ °C was suggested. A retrogressive metamorphic event could be also considered. BALINTONI (1975), described antiperthitic textures on the rims of the recrystallized plagioclase in the migmatites as the result of a "final K-metasomatic effect". UDUBAŞA et al. (1988) described the small-scale decomposition of amphibole under near surface conditions, and zoisite and chlorite remobilization in veinlike forms. He also observed a remobilization of transition metals in sulphide phase.

In this study, since veinlike occurrence of quartz has not been commonly observed, we may consider the silica content as reflecting the premetamorphic content. Further evidence is the absence of pargasite, the silica poor amphibole. In fact, solution transport over large areas can be excluded as neither discordant nor concordant pegmatites occur in the region. The presence of sharp boundaries between the amphibolites and the paragneisses prove that the metasomatic processes were lithologically controlled and supported mainly by the former sedimentary layers which met the conditions for the permeability. The metamorphic events did not change drastically the whole rock chemical composition, the main effect being a major elemental redistribution among the minerals. The recrystallization of the rock in solid state, leading to the change of the former textures has been proven by the existence of zoisite crystals which exceed the limits of the host (UDUBAŞA et al., 1988). However, some elements may have been moved and considering the above reported metasomatic events alkalis should not be used as rock type discriminators. Since not all the elements were influenced during the time in which the system was opened, a global approach of mass balance equations would eventually identify the processes responsible for the original chemical variation.

Analytical techniques

We examined 33 samples of amphibolites and 11 of acidic rocks (paragneisses and augen gneisses) from both formations. Sampling avoided highly tectonized areas. The sample numbers and locations are shown in figure 2. From each sample, 2 kg were granulated in a jaw crusher. The gravel was split into 0.5 kg portions and ground in an agate mill.

Major elements and Zn, Cu, Ni, Cr, V, Zr, Y, Rb, Sr, Ba, Nb were determined by X-ray fluorescence (TOGASHI, 1989) on a sequential X-ray spectrometer system with a Sc–Mo tube at the Geological Survey of Japan, on aliquots of 0.6 and 3 grams, respectively. Co, Sc, Cs, La, Ce, Nd, Sm, Eu, Tb, Tm, Yb, Lu, Hf, Ta, Th, U were determined by INAA. The 0.3 grams aliquots were irradiated on a TRIGA-II Reactor at Rikkyo University, Japan. The gamma ray counting was performed at Rikkyo University and Nagoya University, Japan. REE, with the exception of Dy and Ho, were determined by ion chromatography, on aliquots of 0.5 grams, using the methodology of ASAHARA et al. (1995), at Nagoya University.

The concentration of major and trace elements for amphibolites, according to their location, is given in tables 1, 2 and 3. The chemical composition of thin layers (of centimeters order) of amphibolites interbedded with gneisses from the Topolog Formation together with augen gneisses from both formations is given in table 3.

Results and discussion

MAJOR ELEMENTS

A general view of the variation of oxide concentrations with silica is shown in figure 3. The SiO_2 content of the amphibolites from the Cumpăna Group, between 42–58% (Tabs 1, 2, 3) shows a basic chemical character of the premetamorphic rocks. Their mafic appearance is consistent with the total iron content, expressed as Fe_2O_3 with a mean value of 10.3% and MgO content with a mean value of 7.2%, excluding sample 1 with an outlying value of 23.18%. The ranges of TiO_2 and

Tab. 1 Chemical composition of the amphibolites from the Cumpăna Formation. Concentrations in weight % for major elements and ppm for trace elements. Major elements concentrations were determined by XRF and trace elements by INAA. REE were determined by ion chromatography and INAA.

Sample	1	4	6	11	13	14	17	18	21	22	30	31	35	36	48	50	91	103	105
SiO_2	47.11	47.04	51.73	50.51	53.59	55.09	46.20	46.65	48.70	48.97	51.69	49.42	50.73	56.58	45.33	49.60	46.85	45.82	47.86
TiO_2	0.67	0.28	0.85	1.23	1.36	1.54	2.24	2.25	1.64	1.57	1.68	0.83	1.13	0.87	2.05	0.91	0.19	2.60	2.83
Al_2O_3	5.96	18.63	16.90	15.49	18.04	17.95	15.62	15.76	14.11	14.04	13.86	13.68	16.22	16.46	13.15	16.11	19.64	12.45	14.49
Fe_2O_3*	13.42	7.87	9.45	9.90	8.61	8.82	12.54	12.56	12.94	12.86	12.73	9.65	9.51	6.50	15.52	9.57	5.97	15.71	13.77
MnO	0.23	0.11	0.12	0.15	0.12	0.13	0.16	0.15	0.19	0.17	0.20	0.13	0.15	0.11	0.22	0.15	0.09	0.21	0.19
MgO	23.18	9.90	6.63	7.37	4.15	3.29	5.28	5.88	6.91	7.60	5.87	10.40	7.03	4.49	8.02	8.31	8.94	7.79	6.18
CaO	2.47	9.73	8.71	9.66	6.05	4.49	10.36	9.41	11.69	10.78	9.39	11.93	10.53	5.60	10.68	10.42	12.83	11.07	9.81
Na_2O	0.01	2.53	3.13	2.81	4.42	3.91	3.67	3.77	2.24	1.77	3.00	1.95	3.15	4.44	2.93	2.32	1.31	2.42	3.09
K_2O	0.01	1.24	0.81	1.03	1.09	1.94	1.17	1.23	0.40	0.68	0.34	0.32	0.76	2.75	0.34	0.37	1.71	0.27	0.41
P_2O_5	0.18	0.02	0.24	0.16	0.14	0.12	0.27	0.29	0.14	0.16	0.19	0.04	0.19	0.17	0.17	0.15	-	0.20	0.38
H_2O^+	4.20	2.23	0.95	1.46	1.92	2.61	1.81	1.64	0.65	1.19	0.85	1.26	0.43	0.96	1.17	1.66	1.98	0.92	0.85
H_2O^-	1.80	0.18	0.12	0.13	0.28	0.21	0.27	0.12	0.14	0.10	0.15	0.11	0.08	0.18	0.26	0.36	0.26	0.05	0.07
Sc	13.4	13.9	28.7	38.6	26.4	25.3	32.4	32.9	43.9	41.3	50.1	50.9	44.1	19.5	52.0	38.9	24.6	56.9	34.4
V	30	84	187	299	147	130	261	258	330	338	314	250	268	141	407	260	104	536	301
Cr	1176	251	406	282	144	92	71	54	199	265	58	620	352	121	192	565	536	106	119
Co	120	48	34	38	23	22	43	46	53	52	34	42	44	23	54	40	39	46	41
Ni	739	204	47	40	36	35	41	35	75	88	39	76	30	22	82	59	106	48	41
Cu	10	6	14	7	21	27	50	30	116	80	30	31	16	5	15	27	36	41	27
Zn	130	79	172	97	112	124	103	112	91	125	121	98	82	86	160	105	47	150	118
Rb	1	40	20	17	26	62	22	25	13	15	12	4	17	81	6	5	56	1	3
Sr	16	490	321	265	369	369	217	144	232	231	127	504	406	198	215	288	365	198	279
Y	11	8	32	32	28	42	30	28	31	28	41	19	22	30	51	24	5	59	33
Zr	80	40	87	148	604	627	162	165	113	103	136	37	87	241	101	56	11	103	200
Nb	3.9	2.2	6.9	9.3	19.1	21.6	26.6	31.4	10.2	11.7	4.4	3.9	5.4	7.3	3.5	6.6	2.5	3.8	23.1
Cs	0.3	1.2	0.5	0.3	1.8	1.1	0.5	0.9	0.4	0.6	0.4	0.6	1.8	0.3	0.6	1.4	2.4	-	-
Ba	10	265	473	432	871	1250	213	221	40	34	174	129	192	424	190	241	579	53	134
La	7.7	6.7	27.7	24	43.7	95.4	16.4	18.5	8.8	7.0	9.2	6.7	10.2	16.4	7.3	13.9	1.5	3.8	19.7
Ce	19.2	17.7	63.4	68.3	92.0	186.8	37.3	40.5	21.6	18.7	24.6	18.5	26.6	36.2	18.6	34.1	4.2	12.9	46.0
Pr	2.2	1.6	8.2	9.5	6.7	24.7	4.6	4.6	2.6	2.5	3.2	2.4	2.7	4.1	2.6	4.2	0.5	1.9	5.2
Nd	10.7	5.9	39.4	43.0	36.0	80.3	18.9	20.2	11.0	12.2	16.2	14.0	13.9	19.4	14.5	19.8	2.8	11.9	24.7
Sm	2.34	1.12	6.37	6.32	6.47	14.25	4.74	4.50	3.97	3.39	4.18	3.90	3.83	4.61	5.30	4.20	0.87	4.67	7.26
Eu	0.49	0.47	1.19	1.43	2.46	2.80	1.56	1.46	1.42	1.22	1.33	1.35	1.31	1.24	1.87	1.17	0.34	1.57	2.17
Gd	2.07	1.38	4.97	4.70	6.22	12.04	6.07	4.69	4.97	4.37	4.97	4.35	1.60	4.42	5.80	4.30	0.99	5.52	6.90
Tb	0.43	0.21	0.91	0.86	0.80	1.86	0.87	0.70	0.82	0.68	0.91	0.52	0.66	0.74	1.00	0.67	0.19	0.80	1.12
Er	1.69	0.79	3.38	3.38	3.42	4.70	3.00	2.48	1.91	3.15	3.80	2.13	3.15	3.20	3.38	3.20	0.90	2.93	2.59
Tm	0.22	0.10	0.40	0.44	0.43	0.62	0.35	0.33	0.20	0.42	0.60	0.29	0.40	0.40	0.45	0.39	0.10	0.37	0.40
Yb	1.43	0.66	2.53	2.93	3.40	4.20	2.20	2.30	1.30	2.83	3.70	1.98	2.10	3.01	3.08	2.20	0.65	2.42	1.98
Lu	0.21	0.10	0.40	0.45	0.50	0.60	0.27	0.30	0.11	0.41	0.50	0.30	0.30	0.46	0.40	0.30	0.10	0.36	0.28
Hf	1.6	1.1	2.3	3.9	15.9	16.7	3.6	3.8	3.0	2.6	3.1	1.4	1.8	6.8	2.7	1.6	0.5	3.4	4.7
Ta	0.3	0.2	0.6	0.9	1.3	2.0	2.4	3.0	0.8	0.9	0.4	0.2	0.4	0.9	0.2	0.4	0.3	0.3	2.0
Th	0.82	6.10	3.56	2.06	12.90	34.50	1.85	2.00	0.30	0.77	0.70	0.32	0.60	2.93	0.30	0.20	0.20	0.30	0.23
U	-	1.6	-	-	1.0	1.2	-	0.4	-	-	1.9	-	0.9	-	-	0.4	0.3	-	-

P_2O_5 are 0.28–2.83% and 0.02–0.38%, respectively, for the amphibolites in the Cumpăna Formation and 0.58–2.21% and 0.08–0.56%, respectively, in the Topolog Formation. They are relatively large for both formations, but the mean values of 1.44, 1.12% TiO_2 and 0.18, 0.13% P_2O_5 are similar to many tholeiites of mobile Proterozoic zones (ZHAO, 1994). The other major oxide concentrations are in the range of basalt variation, although there is a high probability of encountering cumulates and altered samples. For the safe modeling of possible descent lines, it is better to exclude from calculation samples 1, 4, 22, 25, 26, 44 and 91 according to the basaltic screen given by MANSON (1967), figure 4A and the alteration discriminating diagram of HUGHES (1973), figure 4B.

Any attempt to explain these chemical variations should start from the question of the dominant mechanism which caused them. The continuous decrease of magnesium and total iron, while silica is increasing, suggests a preponderant subtraction of these elements, which a fractional crystallization from a common parental magma would explain, although dilution, resulting from an increasing supply of felsic material of constant composition, may have the same effect.

Tab. 2 Chemical composition of the amphibolites from the Topolog Formation. Analytical methods see table 1.

Sample	25	26	44	51	59	63	74	95	99
SiO_2	48.01	42.86	49.52	49.68	54.08	49.40	51.97	55.77	47.00
TiO_2	2.21	1.44	0.72	0.89	0.68	1.11	1.09	0.74	1.83
Al_2O_3	15.12	15.58	16.89	16.26	16.43	18.88	17.29	16.49	15.94
Fe_2O_3*	10.58	13.08	7.79	9.46	7.14	9.47	9.02	6.75	12.20
MnO	0.16	0.18	0.11	0.15	0.12	0.13	0.12	0.11	0.18
MgO	6.07	8.54	8.99	8.25	6.11	5.21	5.70	5.45	6.79
CaO	10.66	15.13	10.90	10.49	8.81	9.80	8.08	8.05	9.72
Na_2O	2.03	0.76	2.43	2.38	4.10	3.89	3.56	4.15	3.31
K_2O	1.87	0.59	0.75	0.38	1.24	0.77	1.34	1.27	0.74
P_2O_5	0.56	0.10	0.11	0.17	0.08	0.14	0.09	0.12	0.44
H_2O^+	2.6	1.77	1.23	1.45	0.98	1.41	1.69	0.69	1.36
H_2O^-	0.24	0.20	0.32	0.10	0.08	0.08	0.22	0.11	0.26
Sc	21.1	50.6	30.2	37.7	30.9	25.9	27.8	28.7	39.8
V	190	322	192	253	223	290	292	182	269
Cr	229	478	565	545	76	67	112	90	174
Co	38	52	39	37	27	29	38	30	44
Ni	113	102	100	58	31	31	60	42	20
Cu	39	10	26	28	5	69	67	41	25
Zn	55	112	66	100	57	79	74	59	113
Rb	77	17	18	2	48	21	38	54	18
Sr	593	540	267	296	248	658	393	266	456
Y	28	26	20	25	24	13	20	27	33
Zr	155	88	439	57	79	45	76	116	101
Nb	34.5	8.8	9.2	7.0	5.3	4.8	3.2	5.5	7.4
Cs	1.0	0.4	0.8	0.6	0.7	0.5	0.5	0.9	0.8
Ba	331	60	240	241	83	239	271	133	213
La	19.7	5.9	13.9	13.9	13.2	7.8	12.0	13.9	17.4
Ce	62.8	18.7	28.1	34.1	28.3	17.1	21.9	33.1	41.5
Pr	7.0	2.3	2.9	4.2	3.4	2.1	2.6	4.3	5.5
Nd	30.3	11.3	12.6	19.8	14.5	10.7	11.9	22.7	28.9
Sm	5.79	2.95	3.00	4.20	3.50	2.50	2.66	4.40	6.38
Eu	2.16	1.03	0.90	1.17	1.11	0.80	0.87	1.40	2.06
Gd	5.80	4.14	2.48	4.74	3.50	2.35	3.04	4.69	6.54
Tb	0.77	0.67	0.43	0.67	0.60	0.30	0.47	0.70	0.84
Er	2.25	3.15	2.35	3.20	2.70	1.13	1.13	3.60	3.04
Tm	0.28	0.40	0.32	0.47	0.34	0.15	0.13	0.43	0.40
Yb	1.76	2.57	2.20	2.20	2.40	0.80	0.69	2.90	2.80
Lu	0.27	0.36	0.33	0.30	0.30	0.10	0.10	0.40	0.40
Hf	3.4	2.2	9.9	1.6	2.3	1.4	2.1	3.5	2.9
Ta	3.1	0.7	0.6	0.4	0.6	0.4	0.3	0.5	0.4
Th	4.21	0.57	2.19	0.20	4.30	0.80	2.72	4.60	0.70
U	-	-	-	0.4	1.7	0.5	-	1.4	0.5

The compatible relationship between major elements and mineral phases allows an easy recognition of the possible modifications of the system. The evaluation of the major oxides variation trends is the interpretation of the least square estimates to a set of mass balance equations, generally written in the form:

$$C_{target,j} = \sum_{i=1}^{n} (X_{iCi,j}) + X_0$$

The expected concentration of element *j* in the basalt *target*, $C_{target,j}$, is specified as a function of the concentrations of element *j* in the mineral and the bulk rock *i*, $C_{i,j}$. The coefficients X_i, which represent the mineral or bulk fractions can then be predicted. The intercept X_0 can be excluded if we want to fit the model through the origin. This makes sense for the case of a simple model like "basalt1 = basalt2 + minerals". In other words, this follows subtraction and/or addition of mineral compositions to a certain bulk composition in order to get another bulk composition. The best model was chosen after scanning the multiple regression coefficients. The fractions and the modal composition of the mineral assemblages which are leaving or entering the magma are quantified at a level for the goodness of fit corresponding to a value of the mean square error (MSE) less than 1. This basically keeps the residuals for individual oxides within the limits of the scattering produced by the analytical error, which is at maximum 10%. Only the alkalis have exceptionally higher residuals which are probably due to a metasomatic event.

Real solutions, having a geochemical meaning, were found for pairs of samples inside the groups which can be regarded as two "lines" of descent: 31, 50, 51, 11, 35, 30, 6, 74 and 48, 103, 17, 18, 99, 105, 21, 63, in figure 5. The basaltic crystallization assemblage consists of olivine, clinopyroxene, plagioclase, magnetite, and ilmenite (see table 4 for the composition of minerals used in calculations, for which the solutions were found). The relevance of their settling is shown by the negative coefficients in determining the target composition (Tabs 5 and 6). In order to assess the trend, the more basic rocks are regarded as more similar in composition to the parental magma.

Recalculating the proportions of the subtracted minerals to 100% of the starting bulk compositions (from the coefficients displayed in tables 5 and 6), the degree of fractionation can be roughly approximated to 17–52% solid fraction. In line 1, samples 50 and 51 descend from 31 whereby 2.2% olivine, 19% clinopyroxene, 3.6% plagioclase and 1.5% magnetite, but the rest of the line appear to be more fractionated, up to 7.6% olivine, 20% clinopyroxene, 16.3% plagioclase and 1.6% magnetite, in sample 30. For line 2, the crystallization is controlled by 2–3.7% olivine, 1.8–17% clinopyroxene, 0–7.5% plagioclase, 0–4.9% magnetite, and 0–2.6% ilmenite. In the calculation magnetite played also the role of adjusting the FeO/MgO in the olivine and pyroxene. The proportion of the bulk composition 48 in determining the composition of 103 is less than 1, requiring an addition of material. This can be seen in the pyroxene solution, having a coefficient of +0.06, which is obviously inconsistent with subtraction. A similar small discrepancy was met in calculating the composition of sample 21. Changing the mineral testing assemblage gave negative

Tab. 3 Composition of thin (cm order) amphibolite layers from the Topolog Formation and some gneisses from both formations. M1, M5, M7, M10 and M11 are amphibolites interbedded with the gneisses M2, M3, M4 and M6 (Topolog Formation). GNO, H1, H2 and H3 are augen gneisses and b2, f7 and s20 are paragneisses (both formations). See map for location, for the respective areas marked with M, G, H, B, F, S. The concentrations are given in weight % for major elements and ppm for trace. Major elements concentrations were determined by XRF and trace elements by INAA.

Sample	M1	M2	M3	M4	M5	M6	M7	M10	M11	GNO	H1	H2	H3	b2	f7	s20
SiO_2	50.79	65.07	74.92	70.19	57.43	65.91	57.49	52.69	55.44	76.16	70.25	60.74	69.73	65.98	69.6	52.58
TiO_2	1.52	0.83	0.18	0.36	0.58	0.65	0.78	1.17	0.94	0.10	0.39	1.13	0.29	0.83	.30	1.83
Al_2O_3	14.58	15.73	13.32	13.75	16.10	15.33	16.36	16.59	15.41	12.70	15.38	16.79	15.83	14.97	15.55	18.7
Fe_2O_3*	10.87	5.44	1.81	3.51	6.12	4.79	6.65	9.19	7.71	1.68	2.50	7.30	2.12	5.26	2.17	9.63
MnO	0.27	0.07	0.05	0.04	0.11	0.06	0.10	0.14	0.13	0.03	0.03	0.12	0.03	0.09	0.03	0.13
MgO	6.92	2.06	0.30	0.91	5.23	1.80	4.27	5.38	5.65	0.17	0.78	3.03	0.66	1.83	0.55	3.84
CaO	9.43	2.44	1.35	3.01	7.96	4.51	5.79	8.42	8.14	0.61	1.74	2.75	1.05	2.35	1.58	5.68
Na_2O	2.81	3.12	4.31	3.90	3.85	3.26	3.58	3.77	3.75	2.90	3.49	4.11	3.44	4.08	2.64	3.94
K_2O	1.03	3.62	3.34	2.97	1.02	1.77	3.08	1.06	1.43	4.54	3.95	1.38	5.24	1.67	6.24	1.37
P_2O_5	0.18	0.21	0.03	0.06	0.08	0.13	0.11	0.13	0.10	0.22	0.20	0.09	0.18	0.10	0.18	0.14
Sc	36.7	15.5	3.3	5.1	25.3	15.7	24.2	30.7	31.6	2.8	5.4	18.4	3.5	12.7	4.6	29.3
Cr	226	80	7	13	229	31	32	147	121	29	23	172	26	101	14	122
Co	38.2	12.1	1.4	4.8	22.4	9.4	20.5	26.7	28.7	1.0	3.8	12.7	4.2	12.8	3.0	26.5
Ni	89	23	5	6.6	44	9	12	18	37	6	7	38	9	29	6	44
Cu	53	17	3	3	3	14	9	16	24	3	15	31	3	82	7	23
Zn	128	80	26	29	55	45	52	82	65	36	35	79	38	51	38	92
Rb	46	143	123	129	24	77	145	24	44	220	103	34	122	69	148	37
Sr	165	192	70	218	235	313	236	384	173	32	175	310	173	265	201	440
Y	39	36	24	19	24	36	28	31	28	26	24	32	15	30	21	38
Zr	125	182	118	175	89	201	120	138	75	57	159	257	131	267	129	500
Nb	6.5	15.7	8.5	5.5	4.5	6.1	4.9	6.5	4.5	15.2	11.7	12.4	9.3	16.6	11.0	19.6
Cs	0.3	3.1	1.6	0.6	0.9	1.4	1.2	0.3	0.4	2.6	1.5	1.5	1.1	1.0	1.7	1.0
Ba	173	677	273	430	118	374	413	399	227	106	881	491	892	402	1442	670
La	12.0	35.0	15.0	14.8	12.1	23.8	14.6	15.6	11.1	7.7	16.1	26.8	13.0	37.6	34.0	100.9
Ce	28.7	71.8	38.4	34.4	24.8	49.1	32.1	38.6	25.8	19.9	42.5	58.4	31.4	78.8	68.5	183.3
Nd	19.7	30.3	17.5	12.8	17.1	22.8	18.3	23.0	14.4	14.0	22.9	26.8	13.0	28.3	19.1	72.2
Sm	4.53	6.95	3.43	2.03	3.22	5.23	3.86	4.57	3.60	2.73	3.48	5.08	2.00	6.48	2.96	14.08
Eu	1.30	1.23	0.48	0.66	0.79	1.11	1.11	1.52	0.96	0.29	0.70	1.59	0.53	1.33	0.73	3.62
Tb	1.10	1.30	0.74	0.47	0.70	1.35	0.91	1.05	0.80	0.58	0.77	1.02	0.43	1.11	0.60	2.90
Tm	0.70	0.54	0.64	-	0.31	0.38	0.57	0.46	-	-	-	-	0.23	0.6	0.3	0.77
Yb	3.72	2.91	3.09	1.83	2.49	2.41	2.83	2.56	3.12	2.33	2.55	3.45	1.42	2.86	2.2	4.26
Lu	0.53	0.43	0.47	0.29	0.40	0.34	0.40	0.40	0.44	0.30	0.38	0.51	0.21	0.40	0.30	0.61
Hf	2.9	5.5	3.6	4.6	2.9	5.1	3.9	3.4	2.3	2.4	4.8	7.2	3.8	9.0	6.0	17.0
Ta	0.5	0.9	1.1	0.5	0.6	0.6	0.4	0.4	0.3	1.2	0.9	0.6	0.7	1.0	0.5	1.3
Th	1.73	13.58	13.71	7.31	5.38	7.52	4.74	2.04	3.28	5.65	14.48	19.17	10.69	14.70	13.00	33.00
U	1.1	2.0	3.2	2.2	1.7	2.8	19.5	0.9	0.9	3.0	3.8	2.3	1.6	2.9	2.2	0.5

and positive significances in the same solution, which lead to the idea of magmatic assimilation. Beside the alkalis, which are mobile in the majority of the cases, Ca and Al fractionate differently in these two samples. In contrast to the rest of the samples, where crystallization seems to be controlled by calcic pyroxenes, in samples 103 and 21 the ratio CaO/Al_2O_3 is increasing. If we agree with the assimilation process, then phases with a low CaO/Al_2O_3 are needed to accommodate the observed increasing tendency of this ratio. It is difficult to give a proper interpretation using this kind of calculation when it deals with partial chemical re-equilibration, implicitly with phases of similar composition, because the vectors compensate each other. If an alumina rich phase is assumed to

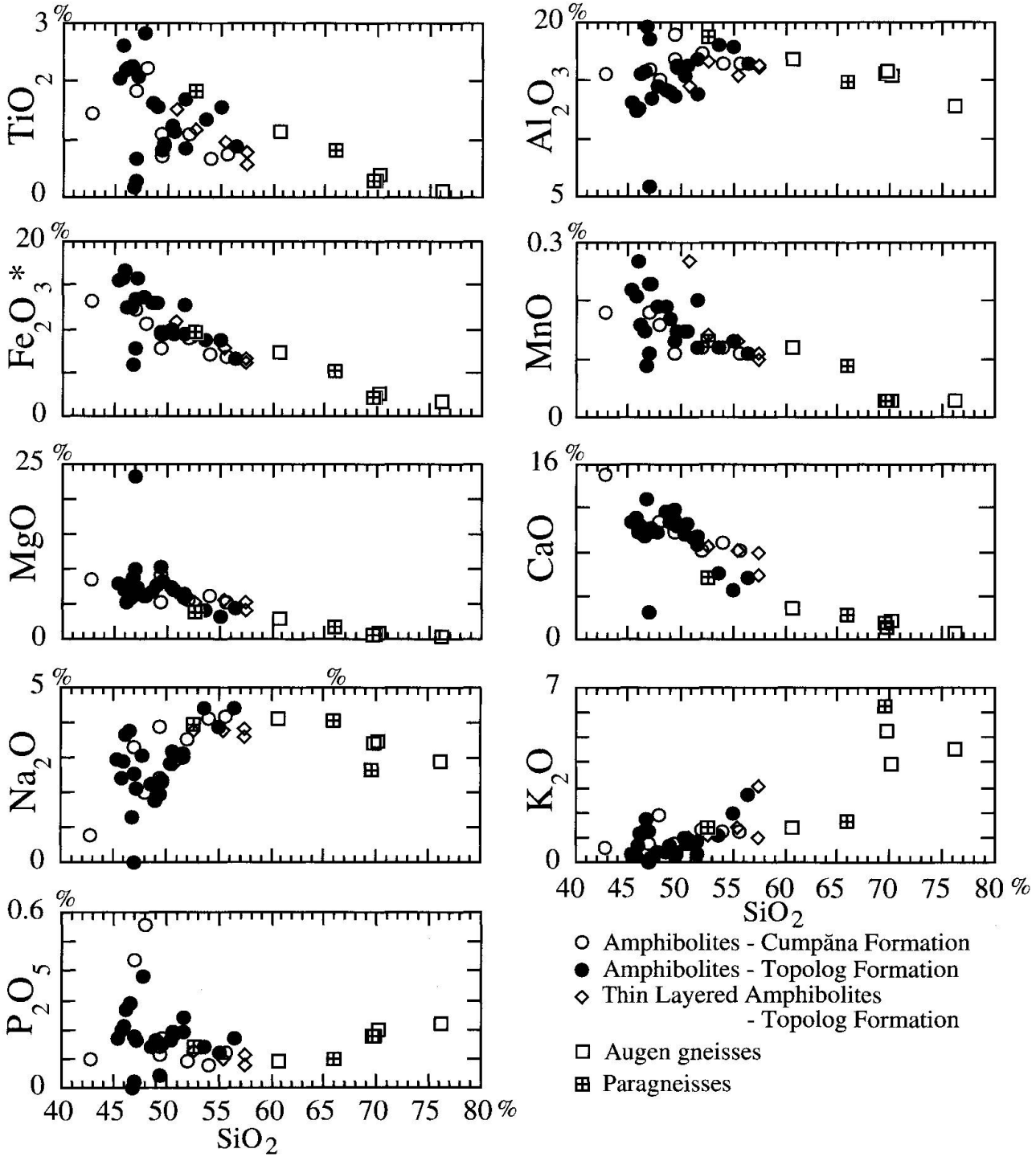

Fig. 3 Variation of major elements versus silica, for amphibolites, paragneisses and augen gneisses from the Cumpăna Group.

be assimilated and cannot equilibrate with the composition of magma, then settling out of an alumina-rich phase would be required. A spinel, an Al-pyroxene, a more sodic plagioclase or a pyralspite garnet can be involved in such a process. Spinels were hardly fitted and the role of plagioclase is not significant. Garnets and high alumina pyroxenes require high pressure and up to this point the constraints upon the state of the system are not fixed.

The oxidation state of the basaltic material, from which the amphibolites were derived, is unknown. Using the relations of SACK et al. (1980) and KILINC et al. (1983) the ratio Fe_2O_3/FeO in the amphibolites seems to cluster around 0.17 at 1200–1400 °C, for the oxygen fugacities of quartz-fayalite-magnetite buffer, at 1 bar total pressure.

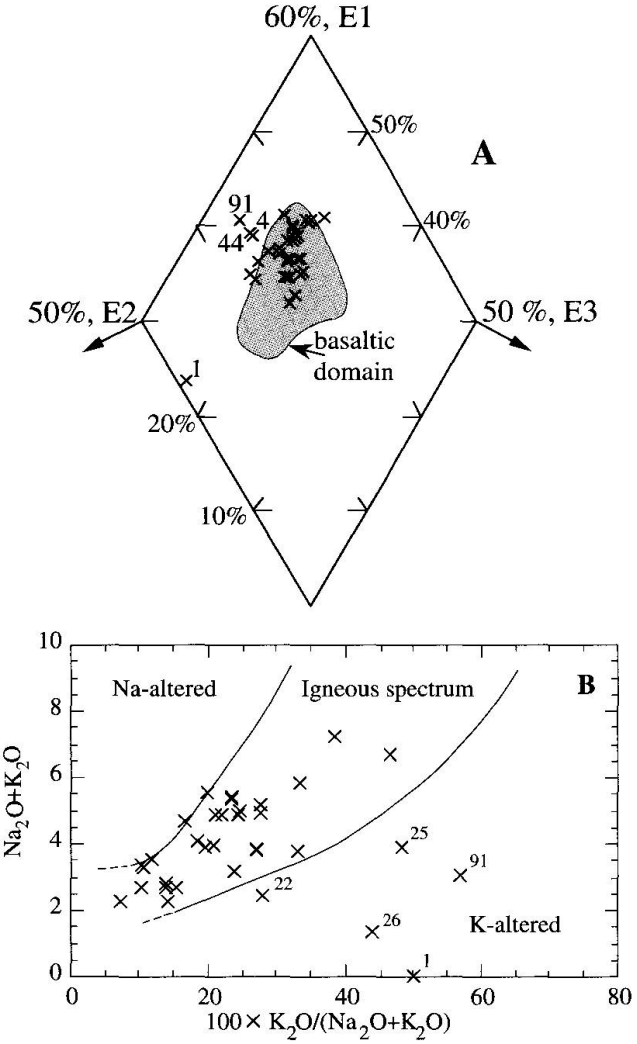

Fig. 4 Position of the amphibolites of this study: A) basaltic screen; the amphibolites compositions were recast using the procedure and factor measurements in determining the composition of the appropriate end member given by MANSON (1967). B) alkali alteration discriminating diagram, after HUGHES (1973).

We shall use this value, which is not very different of that recommended by BROOKS (1976) for the standardization of unknown iron partition in basalts. Sample 31 would have FeO/MgO of 0.72 which is low enough to be considered close to its parental liquid. According to ALBARÈDE (1992) and the references therein, FeO/MgO ratios of primary melts are constrained to the range 0.4–0.8. The concentration of MgO and FeO in the parent can be calculated on the olivine line, using the relations derived by ALBARÈDE (1992), for equilibrium fractionation of olivine,

$$(1-F) = \frac{C_0^{FeO}}{C_{fa}^{FeO}}(1-z^{K_D}) + \frac{C_0^{MgO}}{C_{fo}^{MgO}}(1-z),$$

$$z = FC_0^{MgO}/C_{parent}^{MgO},$$

where C_0 is the concentration of the oxide written in the superscript, in the liquid; subscripts *fa* and *fo* stand for fayalite and forsterite. K_D is the partition coefficient of the ratio FeO/MgO between olivine and liquid. It is assumed constant and equal to 0.3 (ROEDER and EMSLIE, 1970; PEARCE, 1978). Replacing F (the fraction of melt) by $1+S$, where S is the amount of olivine to be added, we solve the above equation, iteratively, with respect to z.

Substituting the value of C^{MgO} found for the parent in the following equation,

$$\left(\frac{C^{FeO}}{C^{MgO}}\right)_{\text{liquid}} = \left(\frac{C^{FeO}}{C^{MgO}}\right)_{\text{parent}} z^{(K_D-1)},$$

(IRVINE, 1977; ALBARÈDE, 1992, 1995), the value of C^{FeO} in the parent is found. Making use of the molar proportions of fayalite and forsterite, determined by the partitioning of FeO/MgO between liquid and solid, we know which type of olivine is crystallizing.

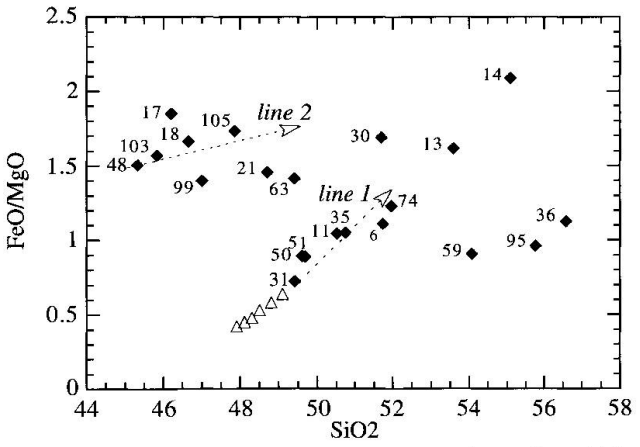

Fig. 5 Differentiation trends on the FeO/MgO vs SiO_2 diagram for the amphibolites from both formations. Possible parents of sample 31 shown as triangles were determined using the equation of ALBARÈDE (1992), (data from Tab. 7).

Tab. 4 Composition of the minerals used in calculations. Sources: a – McKENZIE and O'NIONS (1991); b – DEER et al. (1966).

Mineral	SiO_2	TiO_2	Al_2O_3	FeO*	MgO	CaO	Na_2O	K_2O	source
olivine	40.84	0.02	0.04	9.68	49.53	0.06	0	0	a
clinopyroxene	54.76	0.21	2.59	2.59	17.36	18.34	2.04	0.01	a
plagioclase (An)	44.79	0	34.81	0.27	0.03	19.47	0.64	0	a
quartz	100	0	0	0	0	0	0	0	b
oligoclase	64.1	0	22.66	0.3	0.25	3.26	9.89	0.05	b
microcline	64.46	0	18.55	0.13	0	0.17	0.49	16.07	b
biotite	37.17	3.14	14.6	33.55	4.23	0.17	0.15	8.25	b
magnetite	0.27	0	0.21	92.81	0	0	0	0	b
ilmenite	0.11	48.9	0.54	48.45	0.56	0.65	0	0	b

Tab. 5 Solution of the least square fitting of the major oxides between sample 31 and samples 50, 51, 11, 35, 30, 6 and 74. The calculation used the mineral compositions given in table 4. Note the negative significances of the minerals.

Calculated coefficients for the model: "target sample = sample 31 + minerals"							
sample 31	1.37	1.37	1.63	1.53	1.84	1.9	2.09
olivine	−0.03	−0.03	−0.07	−0.07	−0.14	−0.08	−0.1
clinopyroxene	−0.26	−0.26	−0.36	−0.3	−0.37	−0.53	−0.63
plagioclase	−0.06	−0.05	−0.17	−0.11	−0.3	−0.22	−0.28
magnetite	−0.02	−0.02	−0.04	−0.03	−0.03	−0.05	−0.07
ilmenite	0	0	0	0	0	−0.01	−0.01
target sample nr.	50	51	11	35	30	6	74
MSE	0.03	0.04	0.25	0.41	0.09	0.23	0.69

Tab. 6 Solution of the least square fitting of major oxides between sample 48 and samples 103, 17, 18, 99, 105, 21 and 63. The calculation uses the mineral compositions given in table 4. Note the negative significances of the minerals.

Calculated coefficients for the model: "target sample = sample 48 + minerals"							
sample 48	0.96	1.28	1.41	1.32	1.38	1.09	1.55
olivine	−0.02	−0.04	−0.02	0	−0.04	−0.04	−0.02
clinopyroxene	0.06	−0.16	−0.25	−0.21	−0.16	0.02	−0.35
plagioclase	−0.01	−0.02	−0.06	−0.02	−0.09	0	−0.02
magnetite	0	−0.06	−0.07	−0.06	−0.06	−0.03	−0.11
ilmenite	0.01	−0.01	−0.01	0.02	0	−0.01	−0.04
target sample nr.	103	17	18	99	105	21	63
MSE	0.15	0.32	0.30	0.05	0.17	0.53	0.03

The range of possible parental liquids obtained from such a calculation is given in table 7 and in the FeO/MgO versus SiO_2 plot, figure 5. Using the empirical relationships between MgO, SiO_2 and physical parameters of the magmatic system, of ALBARÈDE (1992), the *P-T* domain is approximated to 1360–1520 °C and 15–22 kbar for their segregation from peridotite. A similar fractional crystallization correction is impossible for sample 48 which is the least fractionated one among the samples fitted on line of descent 2, because of its high ratio FeO/MgO. Apparently, these liquids have a different parent than those from line 1. However, this is difficult to imagine for concordant layers within the same stratigraphic group. Therefore, we may consider an alternative process which can be responsible for producing different lines of descent. Suppose that in a magma chamber, sinking crystals meet the condition of melting and mix with part of the previous residual liquids. If this happens, it is possible to fit the composition of sample 48 by taking 71% of a liquid having the composition of sample 35 and mixing with 2% olivine, 13% clinopyroxene, 4% plagioclase, 7% magnetite and 3% ilmenite. This process will be discussed further, with respect to REE patterns.

Testing the magmatic differentiation model

Tab. 7 Calculated range of parental liquids of sample 31. The range of parental liquids calculated by correction of the olivine crystallization. S is the amount of olivine added to the composition of sample 31, by weight percents.

S %	4	8	12	16	20	24
Forsterite mol%	90.3	91.1	91.9	92.5	93.0	93.4
FeO parent	7.6	7.7	7.7	7.7	7.7	7.6
MgO parent	11.9	13.3	14.6	15.9	17.1	18.2
FeO/MgO parent	0.64	0.58	0.53	0.48	0.45	0.42
SiO_2 parent	49.1	48.8	48.5	48.3	48.1	47.9

Tab. 8 Solution of the least square fitting of major oxides between sample 51 and sample 11, 6, 74, 13, 14, 95 and 36. The calculation is in the same manner as shown in tables 5 and 6. Note the positive significances of the minerals.

Calculated coefficients for the model: "target sample = sample 51 + minerals"							
sample 51	0.88	0.78	0.69	0.46	0.32	0.67	0.45
quartz	0.03	0.01	0.01	0.02	0.04	0.06	0.07
oligoclase	0.03	0.14	0.2	0.38	0.39	0.22	0.28
microcline	0.01	0	0.03	0	0.05	0.04	0.11
biotite	0.05	0.06	0.07	0.13	0.17	0.01	0.06
target sample nr.	11	6	74	13	14	95	36
MSE	0.16	0.01	0.07	0.22	0.56	0.13	0.22

for the samples with more than 52% SiO_2 the misfit becomes very large. Instead, addition of quartz, oligoclase, microcline and biotite to samples fitted on line 1 supports the composition of samples 13, 14, 59, 95 and 36. We can regard these samples as mixtures between the end members of the fractionation, described above, and a sedimentary derived component. Based on least square calculations the amount of the contaminant varies between 12 and 68% (Tab. 8). Large quantities of material are unlikely to be melted in the magma, therefore a relation with sedimentary processes, such as tuff deposition may be considered. Within the same limits, this model was confirmed for the thin layered amphibolites M1, M5, M7, M10 and M11.

MINOR AND TRACE ELEMENTS

It is easier to describe the behavior of minor and trace elements with respect to the compositional trends of major elements, estimated by least square fitting. Thus, three groups can be identified:

I – basalts assumed to be formed due to fractional crystallization (line 1, Fig. 5);

II – basalts assumed to be formed due to fractional crystallization plus magma mixing (line 2, Fig. 5);

III – pyroclastites or samples which confirm a mixing model between an igneous component and a sedimentary one.

These groups have different normalized REE patterns. The first group have $LREE_n$ higher than $HREE_n$, with La_n between 17 and 80. $HREE_n$ display almost parallel horizontal patterns, with a mean enrichment of 10 times the chondritic value (Fig. 6A). The second group exhibits a variation from convex patterns, with La_n between 10 and 20 and consequential depletion of HREE to linear patterns with higher La_n, between 20 and 60 and higher La_n/Lu_n (Fig. 6B). The exception is sample 74 with a high degree of uncertainty (high values for residuals in fitting a simple fractionation model), which was plotted together with the second group, because of its REE similarity with sample 63.

The mass balance equations can be used to predict the abundances of the nonstoichiometric constituents of the phases during crystallization in basalts produced by melting of different sources. Then, the observed abundances can be compared to the predicted ones in order to fit the most probable model. Rare earths are relatively immobile, because of the high charge and high ionic potential so that the observed abundances are supposed to be only a consequence of their igneous fractionation.

From a simple model, which implies batch non-modal melting (SHAW, 1970),

$$C_L = C_0/(D_0 + F(1 - P)),$$

and subsequent Rayleigh fractionation in the

magma chamber (RAYLEIGH, 1896; NEUMANN, 1954)

$$C_L = C_0 F^{(D-1)},$$

the source was found to be a garnet lherzolite at 4–6% of melting. The concentrations of elements in the liquid, C_L, depending on the values in the parent C_0, bulk partition coefficients of solid assemblages D_0, D and proportion of minerals which go into the melt P (the bulk partition coefficient for the assemblage which is melting) at a certain fraction of melt F were calculated using the following:

1. Melting uses olivine, orthopyroxene, clinopyroxene and garnet in the proportions around 13:12:25:50, comprising peritectic melts as suggested by JOHNSON et al. (1990), starting from an original composition of garnet lherzolite (55–70% olivine, 20–25% orthopyroxene, 5–15% clinopyroxene and 5–10% garnet). The partition coefficients for clinopyroxene are those used by HANSON (1980) in modeling the mantle melting.

2. Crystallizing solids are assumed to lie within the limits calculated from the least square fitting of major elements. A representative assemblage consists of 8% olivine, 70% clinopyroxene, 16% plagioclase and 6% magnetite, calculated from samples 31 and 50, normalized to 100% solid. The crystallization is assumed to take place in the uppermost position of the magma chamber, in the lowest temperature zone. The partition coefficients of clinopyroxene are those given by SCHNETZLER and PHILPOTTS (1970) for an andesitic basalt from Japan (all the partition coefficients used in calculations are shown in Tab. 9).

During fractional crystallization, from a parental liquid derived by 5% melting of a garnet lherzolite, LREE are more enriched, than HREE (Tab. 9, Fig. 7). It is important to keep the garnet in the residual solid of the melting mantle in order to fit the Ce/Yb ratio of the observed patterns. This is possible up to 10% degree of partial melting, until garnet is consumed. According to FALLOON et al. (1988), garnet can be stable in peridotite at 20 kb, in hydrous conditions.

These liquids can describe the observed patterns for successive subtractions of solid, between 20% and 80% (FC = 0.2–0.8). A fractionation dominated by clinopyroxene would explain most of the observed patterns, but if the REE patterns of samples on the lines of descent are to be compared from the point of view of fractional crystallization, one can see some nonconcordances. For instance, sample 103, which is more fractionated than 48, considering the major elements composi-

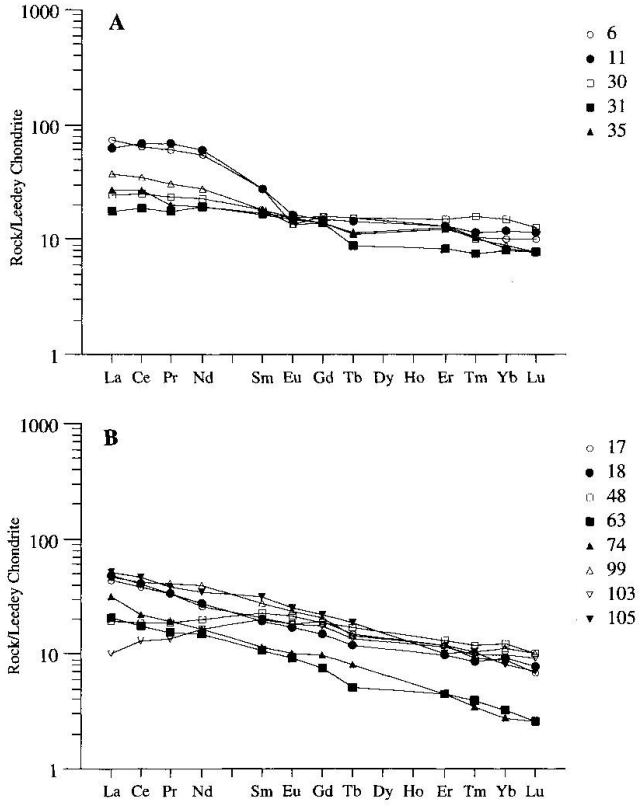

Fig. 6 Chondrite normalized REE patterns of the amphibolites from the Cumpăna Group, arranged according to the trends observed in the major elements concentrations (see also, Fig. 5): 6A shows the samples belonging to group 1 of descent (line 1); 6B shows the samples belonging to group 2 of descent (line 2); the exception is sample 74 with a high degree of uncertainty, which was plotted together with the second group, because of its REE similarity with sample 63. Normalization is to Leedey chondrite (MASUDA et al., 1973; MASUDA, 1975).

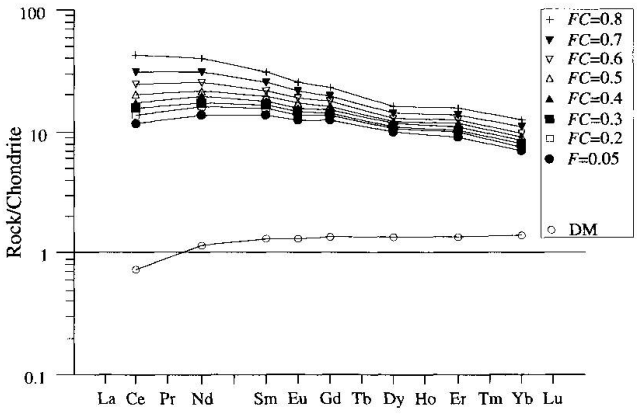

Fig. 7 Normalized REE patterns showing the effect of fractional crystallization of FC% mass of solid from a liquid derived from garnet lherzolite (DM), at 5% batch melting. 2.6% garnet is still present in the mantle and the solid which is crystallizing consists of 8% olivine, 70% clinopyroxene, 16% plagioclase and 6% magnetite, calculated from samples 31 and 50, normalized to 100% solid. Partition coefficients are from table 9.

Tab. 9 Partition coefficients for REE and depleted mantle abundances used in calculations. Calculated REE abundances using a model which involves partial melting, fractional crystallization and resorption of crystals. Partition coefficients are those compiled by HANSON (1980); K_{cpx}* is from SCHNETZLER and PHILPOTTS (1970); the coefficients for magnetite and ilmenite are considered to be close to 0.01, IRVING (1978). The lower values of clinopyroxene were used for melting processes, whereas the higher values were considered to fit the liquid composition during crystallization. The mode of crystallizing assemblage is assumed to be: 8% ol, 70% cpx, 16% pl and 6% mt, which is the least square solution of the best fitted pair on the liquid line, samples 31 and 50, normalized to 100% solid. The composition of Depleted Mantle (DM) is from MCKENZIE and O'NIONS (1991).
Column F = 5% shows the calculated composition of a liquid segregated from DM at 5% non-modal melting. Original mode of the garnet peridotite is: ol-55%, opx-25%, cpx-15%, gar-5%. The mode of melting is 13:12:25:50. Columns *FC* = 20% and *FC* = 90% show the calculated concentrations of REE in the liquid after the crystallization of 20% and 90%. Columns *R* = 0.3 and *R* = 1.7 show the calculated concentrations of REE in the liquid after resorption of a solid with the mode 28% ol, 50% cpx, 16% pl, 6% mt at ratios 0.3 and 1.7 against the residual liquids corresponding to *FC* = 20% and *FC* = 90%, respectively. All concentrations are in ppm.

REE	K_{ol}	K_{opx}	K_{gar}	K_{cpx}	K_{cpx}*	K_{pl}	$K_{mt\text{-}ilm}$	DM	*F* = 5%	*FC* = 20%	*FC* = 90%	*R* = 0.3	*R* = 1.7
Ce	0.0005	0.0030	0.021	0.098	0.208	0.200	0.01	0.722	11.19	13.44	74.22	10.20	15.58
Nd	0.0010	0.0068	0.087	0.21	0.427	0.140	0.01	0.815	9.79	11.39	46.64	8.77	10.60
Sm	0.0013	0.0100	0.217	0.26	0.681	0.110	0.01	0.299	3.17	3.55	10.14	2.75	2.38
Eu	0.0016	0.0130	0.320	0.31	0.635	0.730	0.01	0.115	1.10	1.21	3.01	0.97	0.87
Gd	0.0015	0.0160	0.498	0.30	0.875	0.066	0.01	0.419	3.86	4.20	9.19	3.26	2.20
Dy	0.0017	0.0220	1.060	0.33	0.980	0.055	0.01	0.525	3.85	4.12	7.75	3.21	1.90
Er	0.0015	0.0030	2.000	0.30	0.932	0.041	0.01	0.347	2.32	2.51	5.08	1.95	1.21
Yb	0.0015	0.0490	4.030	0.28	0.896	0.031	0.01	0.347	1.72	1.86	4.00	1.44	0.93

ol = olivine, opx = orthopyroxene, gar = garnet, cpx = clinopyroxene, mt = magnetite, ilm = ilmenite

tion, has lower values for REE. Samples 63 and 74 display very depleted patterns in contrast with the others. Apparently, different degrees of melting of the source could be responsible for such a "disruption" between major elements and REE. The existence of crossing REE patterns suggests the involvement of another mechanism. LANGMUIR et al. (1977) and HANSON (1980) described a "dynamic melting system" characterized by processes like continuous, but incomplete extraction of melt, solidification, remelting and mixing in the magmatic chamber. Taking account of self-resorption of solid particles formed in the melt, MASUDA (1978) explained a possible "backward" fractionation with respect to REE patterns. He gave the following expression to relate the new concentration in the liquid, C_n, after n times resorption of infinitesimal amounts of minerals, ΔW,

$$ln(C_n/C_0) = -(1-k)n\Delta W,$$

to the concentration in the previous melt, C_0; k is the bulk partition coefficient. The following conditions were chosen for calculation:

1. The parental liquid is segregated from garnet lherzolite at 5% melting.

2. The crystallization is controlled by clinopyroxene in the mineral assemblages, settled above.

3. The sinking solids meet the condition of remelting and mix with the previous residual melt. The remelting mode is similar to the solid assemblage which has crystallized that is olivine, clinopyroxene, plagioclase and magnetite in the proportions 8:70:16:6. A significant depletion for the HREE is achieved at 28:50:16:6. More than 28% olivine will not have any notable effects on the concentrations in the resulting liquid. One solution, which can explain how we can get the observed patterns shown in figure 6B, is given in figure 8. In early stages the system has crystallized 20% of its mass. Partial remelting of this solid and a mixing ratio of 0.3 against the previous amount of liquid will produce retrogressive patterns similar to that of sample 103. In the final stages of crystallization, 90% of magma has crystallized. Partial remelting of this solid and mixing with the previous residual melt in proportion of 1.7, can generate a pattern similar to those of samples 63 and 74. The results of calculations are shown in table 9. Such an oscillating crystallization and remelting may occur in a dynamic environment as the magma chamber is ascending intermittently, in keeping with the solidus temperature and pressure (TANAKA, 1975).

Samples 13, 14, 36, 59 and 95 are different from the rocks described so far and exhibit concave patterns with high enrichment values for LREE, between 35 and 260 (Fig. 9). They have similar normalized patterns and abundances to paragneisses (Fig. 10), thought to originate from arenite-lutites (ARION et al., 1986). This obviously supports the previous hypothesis involving mixtures of the compositions of samples on the basaltic de-

scent line and crustal derived sediments. The question is whether they are mechanical mixtures or the products of metamorphic differentiation regarding melting of sediments. Considering that at the time of melting or crystallization C_S/C_L approaches D, we can check on the relation between an amphibolite layer, taken as a solid differentiated from its felsic host considered to be the residual liquid. A predominantly amphibole rich fraction would require bulk partition coefficients greater than 1, for Ce and Yb. D_{Ce} is 1.15 and D_{Yb} is 5.89 for a residue containing 70% amphibole and 30% plagioclase (K_d-values for melting of sediments are from HANSON, 1980, his Tab. 2). The spatially closely related rock suite M1, M2, M5, M6 shares the general characteristics of the third group. In the thin layering sequence, M1 and M5 are the assumed amphibole rich solids and M2, M6, the residual liquids (their compositions are given in Tab. 3). D_{Ce}-values are less than 1 and D_{Yb}-values are around 1. The REE patterns for the sample pairs M1, M2 and M5, M6 do not show a solid-liquid relationship (Fig. 11).

The transition metals Cr, Co, Ni, Cu, and Zn have a more complex behavior due to their high electronegativity. Bonding with non-metals such as sulphur can be predominantly covalent and

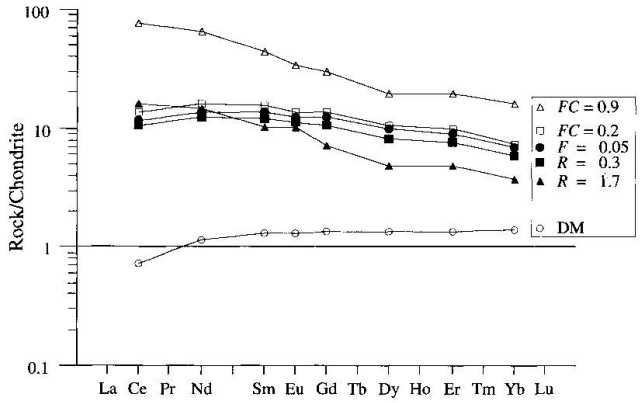

Fig. 8 Normalized REE patterns showing the effect of partial remelting of the solids settled by fractional crystallization. The melting of peridotite is the same as in figure 7. As the crystallization proceeds, the sinking crystals meet the condition of remelting and mix with previous residual melt. $FC = 0.2$ and $FC = 0.9$ indicate the normalized concentrations of REE in the liquid after the crystallization of 20% and 90% of its initial mass. $R = 0.3$ and $R = 1.7$ indicate the normalized concentrations of REE in the liquid after resorption of a solid with the mode 28% ol, 50% cpx, 16% pl, 6% mt at ratios equal to 0.3 and 1.7 against the residual liquids corresponding to $FC = 20\%$ and $FC = 90\%$, respectively. Increments of liquid are allowed to leave the system in order to achieve the required mixing mass ratios between the remelting solid and the former residual liquids. See also table 9.

easy to achieve in metamorphic fluids. For the Cumpăna Group amphibolites, the magmatic fractionation modeling of these elements is rather difficult if we consider their remobilization in sulphide phase during metamorphism. Besides the well-known mobility, GANDRABURA et al. (1992) showed that there is an influence of material of sedimentary origin in the geochemical association of Ni–Co–Cr–Cu, met in some of the amphibolites having an igneous origin. Therefore, an alternative way to recognize a meaningful trend in their abundances is a statistical description of the data. For this purpose, a comparison was made between the samples fitted on the liquid line and thus considered a priori one population and those assumed to be mixtures between igneous and sedimentary components, as a second population. The range of variation, quartiles and the mean values are shown in a box plot, figure 12. Except Ni, the variances and the true mean values of concentra-

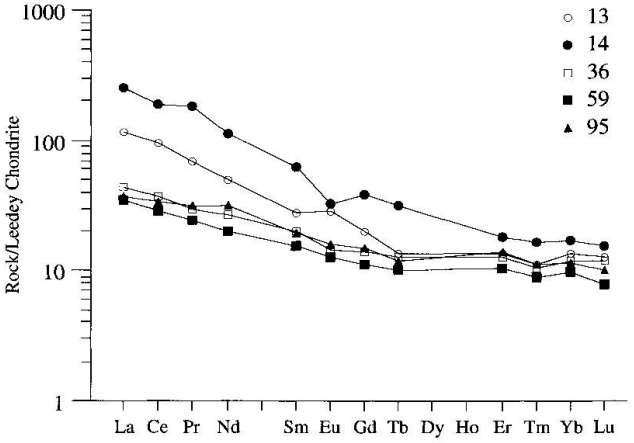

Fig. 9 Normalized REE patterns of the amphibolites from the Cumpăna Group corresponding to those which appear to be mixed with sediments from the view point of major oxide composition (see also Figs 5 and 10).

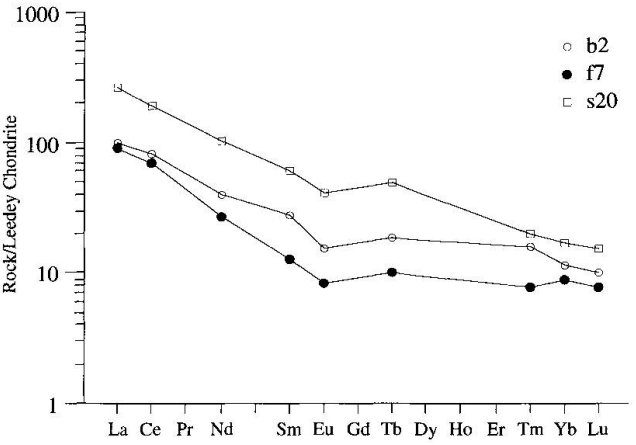

Fig. 10 Normalized REE patterns of paragneisses from the Cumpăna Group; these patterns are given for comparison with those from figure 9.

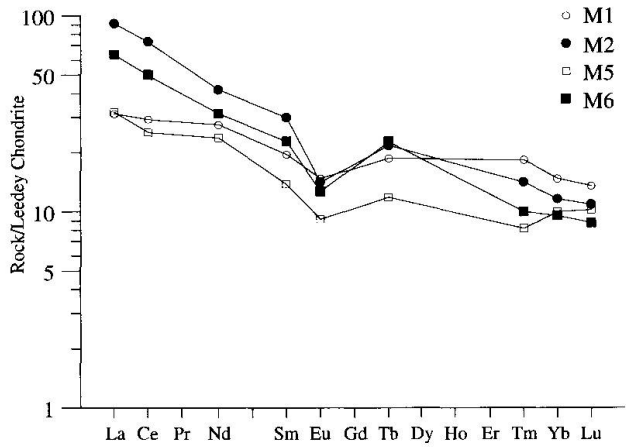

Fig. 11 Normalized REE patterns of thin layered amphibolites from the Topolog Formation; M1 and M5 in contact with amphibole rich gneisses M2 and M6. Assuming that M1 is the solid which remained after the extraction of the liquid M2, from the present knowledge of partition coefficients, one can see that there is no similarity with a relationship between a solid and its cogenetic liquid.

tions for the same metal in the two populations are significantly different at 5% level from the point of view of statistical tests. The mean values are lower for the samples belonging to second population. This can be seen as a dilution effect if the second group is genetically related to the first one. Again, admixture of material with lower concentrations, such as a crustal sediment, can accommodate the observed tendency.

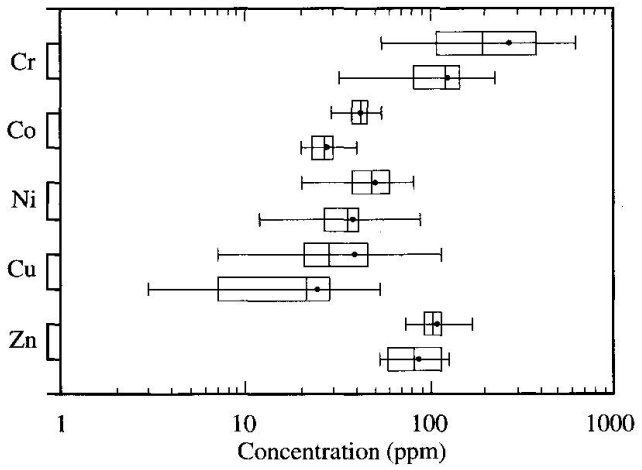

Fig. 12 Box plot showing the distribution of Zn, Cu, Ni, Co and Cr abundances in the amphibolites assumed to have originated from basaltic liquids (upper site) in comparison with those for which we assume an addition of sedimentary material (the lower site). The middle line is the second quartile (the median). The concentrations ranges and mean values (dots) are correspondingly lower in the sedimentary admixed samples.

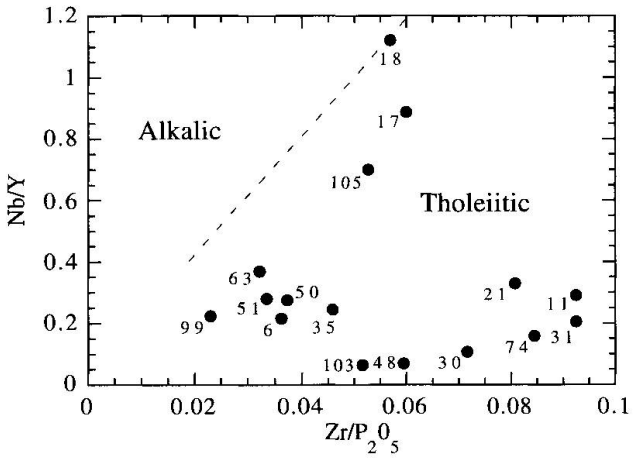

Fig. 13 Discrimination diagram (after WINCHESTER and FLOYD, 1976) showing the tholeiitic character of the amphibolites from the Cumpăna Group.

HFSE, which are relatively immobile, may constrain the original composition of the rocks. Additionally, magmas from a given tectonic setting tend to share patterns of their abundances.

The samples of this study, which are assumed not to be mixed with sediments as could be deduced from the major elements trends and minor and trace elements distribution, were plotted in the $Nb/Y-Zr/P_2O_5$ diagram of WINCHESTER and FLOYD (1976). The result (Fig. 13) indicates a tholeiitic composition. The relative depletions of

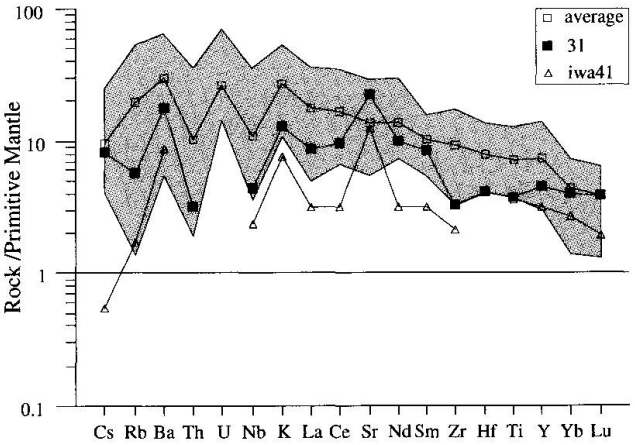

Fig. 14 Primitive mantle normalized concentrations of selected elements in the amphibolites from the Făgăraş Mountains. The shaded area represents the range of concentrations in the amphibolites and the open squares show the averaged values of concentrations; solid squares show the position of sample 31. An island arc tholeiitic basalt from Iwate Volcano, Japan, represented as triangles is given for comparison. Primitive mantle estimates and the island arc tholeiitic basalt concentrations are from TOGASHI et al. (1992) and therein references.

Nb and Zr suggest that the tectonic environment is close to, or in a continental area (DUPUY and DOSTAL, 1984; HOFMANN, 1988).

This is illustrated on an incompatibility diagram in figure 14. A good resemblance was found between the composition of amphibolite 31 and an island arc basalts from Iwate Volcano in Japan, which was used by TOGASHI et al. (1992) to describe the depleted type of island arc tholeiite, figure 14.

Large ion lithophile elements are highly incompatible, but also mobile and require much care for their petrogenetic use. The amphibolites from the Cumpăna Group have scattered concentrations of Rb, Ba, Th, U, K, although a strong enrichment, if compared with pristine materials, can be observed (Fig. 14).

Conclusion

The rocks found in the Cumpăna Group do not represent primary melts because of their relatively high FeO*/MgO ratios and low Ni contents. They are already fractionated and inverse steps on the liquid line were necessary, in order to approximate their parental composition. The sensitive changes in the major element concentrations with the fractionation produced by crystallization, allowed an estimation of proportions of the subtracted minerals. This process was dominated by clinopyroxene, which accounts for approximately 70% of the mass of settled crystals. The concentrations of FeO, MgO and SiO_2 of the parental liquids of sample 31, corrected for olivine crystallization, were possibly in equilibrium with peridotite between 15 and 22 kbar. Garnet should remain in a residual depleted mantle in order to keep a low concentration of heavy rare earths in the melt and a Ce/Yb ratio similar to that observed. This would happen at up to 10% batch melting, initiated in the garnet stability field, which can exist at 20 kb in hydrous conditions. Some samples show a discrepancy between major elements and REE with respect to crystallization, i.e., more primitive basalts in terms of major elements show higher REE concentrations. This can be explained by partial remelting of the crystallizing solid in magma chamber, prior to eruption. The resulting tholeiitic magmas, strongly differentiated on the way up to surface, passed through the crustal basement and a thin sedimentary cover. The position in a near continental setting is suggested by the negative Nb anomaly and the presence of a depleted mantle source. The required hydrous conditions for the existence of garnet may involve a subduction process. The assumed basaltic liquids from which the amphibolites were derived have similar chemical compositions with island arc tholeiites. Mixing processes, different from assimilation, between basalts and crustal rocks were detected. The amount of contaminant has been estimated at between 12–68% and is thought to be a mechanical mixing with sediments which occurred in a tuff-like deposition. The alternation between "igneous" amphibolites, "sedimentary admixed" amphibolites and paragneisses resemble a strato-volcanic structure where lavas, tuffs and sediments occur in a stratigraphic succession. We find it appropriate to consider the features of an incipient island arc environment for the lithostratigraphic group named Cumpăna prior to its metamorphism. We would like to draw attention upon a possible westward evolution of this arc to a more mature stage. LIÉGEOIS et al. (1996) found that the amphibolites from the pre-Alpine basement of one of the Variscan nappes from Danubian system (Fig. 1) display an island arc signature, with three differentiation trends evolving from an early tholeiitic to a more differentiated low-K calc-alkaline one. The existence in the South Carpathians of at least one more zone of Precambrian age, belonging to the same Carpian Supergroup, with island arc features, suggests a single structure which was split by the Paleozoic tectonic events.

Acknowledgements

This work was supported by the Ministry of Education, Science and Culture of Japan.

We are grateful to Dr. S. Togashi from the Geological Survey of Japan for performing the XRF analysis. We thank Dr. Y. Asahara from Nagoya University for assistance during ion-chromatographic analyses, Dr. M. Munteanu and Dr. T. Stafie from the Geological and Geophysical Institute in Romania, for discussions. The valuable suggestions and criticism coming from Prof. I. Mercolli of Bern University, Dr. R. Hänny of Basel University and from an anonymous reviewer are greatly appreciated. We are indebted to Dr. C. Richardson for his patience in revising the English version of this paper.

References

ALBARÈDE, F. (1992): How Deep Do Common Basaltic Magmas Form and Differentiate? Jour. Geophys. Res., 97, B7, 10 997–11 009.

ALBARÈDE, F. (1995): Introduction to Geochemical Modeling. Cambridge University Press, Cambridge, 543 pp.

ARION, M., VELICU, R., ASIMOPOLOS, L. and ASIMOPOLOS, N. (1986): Raport asupra prospecţiunilor geologice executate in Munţii Făgăraş, sectoarele: Rîul Vîlsan – Rîul Doamnei, Arpaş, Nimaia. Arch. Inst. Geol. Geofiz., Bucharest. Unpublished report.

ASAHARA, Y., TANAKA, T. and YAMAMOTO, H. (1995): Analysis of rare-earth elements in rock samples by ion chromatography using α-HIBA as an eluent. Jour. Min. Petrol. and Ec. Geology, 90, 103–108.

BALINTONI, I. (1975): Studiul petrogenetic comparativ al unor migmatite din M-ţii Făgăraş şi Sebeş. Analele Inst. Geol. Geofiz. Rom. XLIV, 133–179.

BALINTONI, I. HANN, H.P., GHEUCĂ, I., NEDELCU, L., CONOVICI, M., DUMITRAŞCU, G. and GRIDAN, T. (1986): Considerations on a Preliminary Structural Model of the Southern Carpathians Crystalline, East of the Olt River. Dări de Seamă Inst. Geol. Geofiz. Rom., 70–71/5, 23–45.

BERZA, T., KRÄUTNER, H.G. and DIMITRESCU, R. (1983): Nappe structure of the Danubian Window of the Central South Carpathians. Analele Inst. Geol. Geofiz. Rom., 60, 31–34.

BERZA, T., BALINTONI, I., IANCU, V., SEGHEDI, A. and HANN, H.P. (1994): South Carpathians. Romanian Journal of Tectonics and Regional Geology, vol. 75, Suppl. 2, nr. 2, 37–49.

BROOKS, C.K. (1976): The Fe_2O_3/FeO ratio of basalt analyses: an appeal for a standardized procedure. Bull. Geol. Soc. Denmark, 25, 117–120.

DEER, W.A., HOWIE, R.A. and ZUSSMAN, J. (1966): An Introduction to the Rock Forming Minerals (2d ed.). Longman Scientific and Technical 1992, 696 pp.

DIMITRESCU, R. (1964): Studiul geologic şi petrografic al părţii de est a Masivului Făgăraş. Analele Com. Geol. Rom., XXXIII, 153–212.

DIMITRESCU, R. (1978): Structure géologique du massif cristallin Făgăraş-Ezer-Leaota. Revue Roumaine Geol. Ser. Geol., 22, 43–51.

DIMITRESCU, R., ŞTEFĂNESCU, M., RUSU, A. and POPESCU, B. (1978): Geological Map 1:50 000 – 109d-Nucşoara-Iezer-L-35-86-C. Inst. Geol. Geofiz. Rom., Bucharest.

DIMITRESCU, R., HANN, H.P., GHEUCĂ, I., ŞTEFĂNESCU, M., SZASZ, L., MĂRUNŢEANU, M., ŞERBAN, E. and DUMITRAŞCU, G. (1985): Geological Map 1:50 000 – 109c-Cumpăna-L-35-86-D: Inst. Geol. Geofiz. Rom., Bucharest.

DIMITRESCU, R. (1988): Eléments structureaux préalpins dans le massif cristallin de Făgăraş: Dări de Seamă ale Inst. Geol. Geofiz. Rom., 72–73/5, 59–68.

DUPUY, C. and DOSTAL, J. (1984): Trace element geochemistry of some continental tholeiites. Earth Planet. Sci. Lett., 67, 61–69.

FALLOON, T.J., GREEN, D.H., HATTON, C.J. and HARRIS, K.L. (1988): Anhydrous Partial Melting of a Fertile and Depleted Peridotite from 2 to 30 kb and Application to Basalt Petrogenesis. Jour. Petrol., 29/6, 1257–1282.

GANDRABURA, E., DRĂGUŞANU, C. and STAFIE, T. (1992): Some Geochemical Aspects of the Amphibolites from Zarna Valley, Făgăraş Mountains, Southern Carpathians. An. St. Univ. "Al. I. Cuza" Iaşi, XXXVIII–XXXIX/ sII, 201–211.

GHEUCĂ, I. (1988): Versantul sudic al Munţilor Făgăraş. Litostratigrafie şi tectonică. Dari de Seamă Inst. Geol. Geofiz. Rom., 72–73/5, 93–117.

GHIKA-BUDEŞTI, S. (1940): Les Carpates Méridionales Centrales, Recherches pétrographiques et géologiques entre Parîng et le Negoi. Analele Inst. Geol. Rom., XXII, 175–220.

HANSON, G.H. (1980): Rare Earth Elements in Petrogenetic Studies of Igneous Systems. Ann. Rev. Earth Planet. Sci. 8, 371–406.

HOFMANN, A.W. (1988): Chemical differentiation of the Earth: the relationship between mantle, continental crust and oceanic crust. Earth Planet. Sci. Lett. 90, 297–314.

HUGHES, G.J. (1973): Spilites, keratophires and the igneous spectrum. Geol. Mag., 109, 513–527.

IRVINE, T.N. (1977): Definition of primitive liquid compositions for basic magmas. Carnegie Inst. Washington Year Book, 76, 454–461.

IRVING, A.J. (1978): A review of experimental studies of crystal/liquid trace element partitioning. Geochim. Cosmochim. Acta 42/2, 743–770.

JOHNSON, K.T.M., DICK, H.J.B. and SHIMIZU, N. (1990): Melting in the Oceanic Upper Mantle. An Ion Microprobe Study of Diopsides in Abyssal Peridotites: Jour. Geophys. Res. 95, B3, 2661–2678.

KILINC, A., CHARMICHAEL, I.S.E., RIVERS, M.L. and SACK, R.O. (1983): The Ferric-Ferrous Ratio of Natural Silicate Liquids Equilibrated in Air. Contrib. Mineral. Petrol., 83, 136–140.

KRÄUTNER, H.G. (1980): Lithostratigraphic Correlation of Precambrian in the Romanian Carpathians. An. Inst. Geol. Geofiz., v. LVII, 229–296.

LANGMUIR, C.H., BENDER, J.F., BENCE, A.E. and HANSON, G.N. (1977): Petrogenesis of Basalts from the Famous Area: Mid-Atlantic Ridge. Earth Planet. Sci. Lett., 36, 133–156.

LIÉGEOIS, J.P., BERZA, T., TATU, M. and DUCHESNE, J.C. (1996): The Neoproterozoic Pan-African basement from the Alpine Lower Danubian nappe system (South Carpathians, Romania). Precambrian Research 80, 281–301.

MANILICI, V. (1955): Cercetari petrografice şi geologice în regiunea Rîul Doamnei Rîul Cernat. Dări de Seamă Com. Geol., v. XXXIX., 231–250.

MANSON, M. (1967): Geochemistry of Basaltic Rocks: Major Elements. In: HESS, H.H. and POLDERVAART, A. (eds): Basalts. The Poldervaart Treatise on Rocks of Basaltic Composition. Vol. 1 John Wiley and Sons, Interscience Publishers, New York, 215–269.

MASUDA, A., NAKAMURA, N. and TANAKA, T. (1973): Fine structures of mutually normalized rare-earths patterns of chondrites. Geochim. Cosmochim. Acta, 37, 239–248.

MASUDA, A. (1975): Abundances of monoisotopic REE, consistent with the Leedey chondrite values. Geochem. Jour. 9, 183–184.

MASUDA, A. (1978): Effect of continuous self-resorption of solid particles formed in the melt on rare-earth pattern: a possible backward fractionation. Geochem. Jour., 12, 133–135.

MCKENZIE, D. and O'NIONS, R.K. (1991): Partial Melt Distribution from Inversion of Rare Earth Element Concentrations. Jour. Petrol., 32/5, 1021–1091.

MUNTEANU-MURGOCI, G. (1907): Sur l'existence d'une grande nappe de recouvrement dans les Carpates Méridionales. Bul. Soc. Stiinte, v. XVI, Bucureşti, 50–52.

NEUMANN, H., MEAD, J. and VITALIANO, C.J. (1954): Trace element variations during fractional crystallization as calculated from the distribution law. Geochim. Cosmochim. Acta, 6, 90–99.

PEARCE, T.H. (1978): Olivine fractionation equations for basaltic and ultrabasic liquids. Nature, 276, 21/28, 771–774.

RAYLEIGH, J.W.S. (1896): Theoretical considerations respecting the separation of gases by diffusion and similar processes. Philos. Mag. 42, 77–107.

ROEDER, P.L. and EMSLIE, R.F. (1970): Olivine-Liquid Equilibrium. Contrib. Mineral. Petrol., 29, 275–289.

SACK, R.O., CARMICHAEL, I.S.E., RIVERS, M. and GHIORSO, M.S. (1980): Ferric-Ferrous Equilibria in Natural

Liquids at 1 Bar. Contrib. Mineral. Petrol., 75, 369–376.

SĂNDULESCU, M. (1984): Geotectonica României. Ed. Tehn., Bucureşti, 336 pp.

SHAW, D.M. (1970): Trace element fractionation during anatexis. Geochim. Cosmochim. Acta, 34, 237–243.

SCHNETZLER, C.C. and PHILPOTTS, J.A. (1970): Partition coefficients of rare-earth elements between igneous matrix material and rock-forming mineral phenocrysts–II. Geochim. Cosmochim. Acta, 34, 331–340.

STRECKEISEN, A. (1934): Sur la tectonique des Carpates Méridionales. An. Inst. Geol. Rom., XVI, 327–417.

TANAKA, T. (1975): Geological Significance of Rare Earth Elements in Japanese Geosynclinal Basalts. Contrib. Mineral. Petrol., 52, 233–246.

TOGASHI, T. (1989): Determination of major elements in igneous rocks using Sc/Mo dual anode tube, XRF analytical report 1/89. Open-file Report of Geological Survey of Japan, No. 132, 35 pp.

TOGASHI, T., TANAKA, T., YOSHIDA, T., ISHIKAWA, K., FUJINAWA, A. and KURASAWA, H. (1992): Trace elements and Nd–Sr isotopes of island arc tholeiites from frontal arc of Northeast Japan. Geochem. Jour., 26, 261–277.

UDUBAŞA, G., HÂRTOPANU, P., HÂRTOPANU, I., GHEUCĂ, I. and DINICĂ, I. (1988): The metamorphosed copper-nickel mineralizations from the Vîlsan Valley, Făgăraş Mountains. Dări de Seamă Inst. Geol. Geofiz. Rom., 72–73/2, 283–312.

UDUBAŞA, S., NEUBAUER, F. and ŢOPA, D. (1994): Preliminary estimations of the P-T conditions of the metamorphism in the southern part of the Făgăraş Mts. Romanian Jour. Tectonics Reg. Geol. 75/ Suppl. 1, 60–61.

WINCHESTER, J.A. and FLOYD, P.A. (1976): Geochemical magma type discrimination: application to altered and metamorphosed basic igneous rocks. Earth Planet. Sci. Lett. 28, 459–469.

ZHAO, J.X. (1994): Geochemical and Sm–Nd isotopic study of the amphibolites in the southern Arunta Inlier, Central Australia: evidence for subduction at a Proterozoic continental margin. Precambrian Research, 65, 71–94.

Manuscript received April 7, 1997; revised manuscript accepted July 26, 1997.